Published in final edited form as:
Circulation. 2012 May 15; 125(19): 2334–2342. doi:10.1161/CIRCULATIONAHA.111.073239.

Magnetic Resonance Imaging with Three-Dimensional Analysis of Left Ventricular Remodeling in Isolated Mitral Regurgitation: Implications beyond Dimensions

Chun G. Schiros, MEE, MPS[1], **Louis J. Dell'Italia, MD**[2,3], **James D. Gladden, PhD**[3], **Donald Clark III, MD**[3], **Inmaculada Aban, PhD**[4], **Himanshu Gupta, MD**[2,3], **Steven G. Lloyd, MD**[2,3], **David C. McGiffin, MD**[3], **Gilbert Perry, MD**[2], **Thomas S. Denney Jr., PhD**[1], and **Mustafa I. Ahmed, MD**[3]

[1]Samuel Ginn College of Engineering, Dept of Electrical & Computer Engineering, Auburn University, Auburn, AL

[2]Birmingham Veteran Affairs Medical Center, Birmingham, AL

[3]Dept of Medicine, Division of Cardiovascular Disease, University of Alabama at Birmingham, Birmingham, AL

[4]Department of Biostatistics, University of Alabama at Birmingham, Birmingham, AL

Abstract

Background—Although surgery is indicated in patients with mitral regurgitation (MR) when left ventricular (LV) end-systolic (ES) dimension (D) is >40mm, LV ejection fraction (EF) may decrease post-mitral valve surgery. We hypothesize that significant LV remodeling pre-surgery is not reflected by standard echocardiographic parameters measured at the base of the heart.

Methods and Results—94 patients (54±11 years, 38% female) with degenerative isolated MR underwent cine-magnetic resonance imaging (MRI) with tissue tagging and three-dimensional analysis. In 51 control subjects (44±14 years, 53% female), the relation between LVES volume (V) and LVESD was quadratic, while in 94 MR patients this relation was cubic, indicating greater increase in LVESV per LVESD amongst MR patients. Moreover, MRI LVESV from summated serial short axis slices was significantly greater than LVESV using the Bullet formula in MR patients, attributed to a more spherical remodeling distal to the tips of the papillary muscles ($P<0.001$). 35 patients underwent mitral valve repair per current guideline recommendations. LVEF decreased from 61±7 to 54±8 % ($P<0.0001$) and maximum shortening decreased significantly below normal at 1-year post-operatively ($P<0.0001$). Despite normalization of LV stroke volume and LV end-diastolic volume/mass ratio, there was persistent significant increase in distal LVES three-dimensional radius/wall thickness ratio and LVESV index post-surgery.

Conclusions—Despite apparently preserved LVESD, MR patients demonstrate significant spherical mid to apical LVES remodeling that contributes to higher LVESV than predicted by standard geometry-based calculations. Decreased LV strain post-surgery suggests that a volumetric analysis of LV remodeling and function may be preferred to evaluate disease progression in isolated MR.

Correspondence: Mustafa I. Ahmed, MD, UAB Center for Heart Failure Research, Department of Medicine, Division of Cardiology, University of Alabama at Birmingham, 434 BMR2, 901 19th Street South, Birmingham, Alabama 35294-2180, Tel: 205-934-3969, Fax: 205-996-2586, mahmed@uab.edu.

Conflict of Interest Disclosures: None

Keywords

left ventricular dysfunction; magnetic resonance imaging; mitral valve regurgitation; remodeling; surgery

Introduction

Mitral regurgitation (MR) is a frequent form of valvular disease, representing an important public health burden in the US. An estimated 2–2.5 million people were affected in the year 2000, a number expected to double by 2030 due to population growth and aging.[1–3] Isolated MR from myxomatous degeneration of the mitral valve results in a relatively low pressure form of volume overload, due to excess volume being ejected through a secondary ejection pathway into left atrium. Forward cardiac output in MR is preserved by an increase in left ventricular (LV) stroke volume, mediated by augmentation of LV preload (end-diastolic volume), decreased afterload due to the relatively low pressure ejection pathway into the left atrium, and an increase in adrenergic drive. These mechanisms may serve to preserve LV ejection fraction (EF), even in the face of increasing LV end-systolic (ES) dimension (D), volume and LVES wall stress over time. This may explain why despite adherence to current guideline recommendations,[4,5] postoperative LV dysfunction is not uncommon, and is associated with increased morbidity and mortality.[3,6]

The mechanisms involved in the transition to irreversible cardiomyocyte damage in chronic isolated MR remain elusive. This is compounded by the fact that symptoms of heart failure may be very subtle and LV function and geometry may change significantly in the absence of symptoms. Thus, the success of adherence to echocardiographic guidelines is limited by requirement for very close surveillance, which has most likely contributed to the recent reports that patients with isolated MR are not receiving timely surgery, even with advances of surgical repair and minimally invasive surgery.[7,8] Studies have reported a decrease in LVEF post mitral valve repair for isolated MR,[3, 9–15] utilizing echocardiography with geometric assumptions based on LV dimensions for LVEF measurements. These findings have resulted in a body of evidence supporting recommendation for early surgery in the controversy regarding management of asymptomatic patients with severe MR.[9, 16–18]

It is important to note that echocardiographic follow-up studies in MR have utilized the standard LVESD measured at the tips of the papillary muscles. We hypothesize that extensive LV apical remodeling in MR hearts, beyond the base and tips of the papillary muscles, contributes to an increasing LVES volume (LVESV) that is not appreciated by measuring the LVESD alone. Therefore, in the current investigation, we utilize cine-magnetic resonance imaging (MRI) with tissue tagging and three-dimensional (3D) data analysis to quantitate global and regional LV geometry and function in patients with isolated MR.

Methods

Study Population

Ninety-four patients with moderate to severe MR were recruited from June, 2005 to September, 2010 at the University of Alabama at Birmingham. All patients referred for surgery had LVEF>60% and almost all had LVESD <40mm by referral echocardiography studies and need for surgery was based on conservative clinical judgment of the cardiologist and cardiovascular surgeon at the tertiary referral center. MR severity was documented qualitatively on echocardiogram/Doppler studies as well as quantitatively on cine and tagged MRI in all cases. All patients had coronary angiography before surgery to rule out

significant coronary artery disease. Patients with evidence of significant aortic valve disease or concomitant mitral stenosis were excluded. Thirty-five patients with severe isolated MR (mitral regurgitant volume 54±34 ml, mitral regurgitant volume fraction 38±16 %) secondary to degenerative mitral valve disease were referred for corrective mitral valve (MV) repair. All patients underwent cine MRI with tissue tagging before surgery and 12 months after surgery. Cine MRI with tissue tagging was also performed in 51 control volunteers (mean age 44±14 years, median age 42 years, age range 20 to 70 years) who had no prior history of cardiovascular disease and were not taking any cardiovascular medications. The study protocol was approved by the Institutional Review Boards of University of Alabama at Birmingham and Auburn University. All participants gave written informed content.

Surgery

Thirty-five patients underwent MV repair. MV surgery was performed through a median sternotomy and employed standard hypothermic cardiopulmonary bypass and cold blood cardioplegia. A variety of methods were used to repair the MV including leaflet resection, chordal replacement, or a combination of each, and these patients had implantation of a flexible annuloplasty ring. The adequacy of repair was assessed by intraoperative transesophageal echocardiography.

Magnetic Resonance Imaging

Cine MRI—MRI was performed on a 1.5-T MRI scanner (Signa, GE Healthcare, Milwaukee, Wisconsin) optimized for cardiac imaging. Electrocardiographically gated breath-hold steady-state free precision technique was used to obtain standard (2-, 3-, and 4-chamber long axis and serial parallel short-axis) views using the following typical parameters: slice thickness of the imaging planes 8 mm, field of view 40cm, scan matrix 256 × 128, flip angle 45°, repetition/echo times 3.8/1.6 ms).

3D LV geometric parameters were measured from endocardial and epicardial contours manually traced on cine magnetic resonance images acquired near end-diastole (ED) and ES. The contours were traced to exclude the papillary muscles. The contours at ED and ES were then propagated to the rest of the timeframes using a dual propagation technique.[19] LV volumes were computed by summing up the volumes defined by the contours in each short axis slice multiplied by slice thickness. These volumes were referred to as measured volumes in the current study. LV volume-time curve was constructed and differentiated with respect to time to obtain the peak early filling rate.[19]

The contour data at ED and ES were transformed to a coordinate system aligned along the long-axis of the LV and converted to a prolate spheroidal coordinate system as described previously.[20] The prolate spheroidal coordinate system has one radial coordinate (λ) and two angular coordinates (μ, θ). Cubic B-spline surfaces, $\lambda_{endo}(\mu, \theta)$ and $\lambda_{epi}(\mu, \theta)$, were fit to the λ coordinates of the endocardial and epicardial contours for each time frame. Each surface used 12 control points in the circumferential direction (θ) and 10 control points in the longitudinal direction (μ). The control points of each surface were computed to minimize the following error function,

$$\varepsilon=\sum_{k}[\lambda(\mu_k,\theta_k)-\lambda_k]^2+\gamma S(\lambda)$$

where γ is a weight set to 0.1. The first term in the error function is the squared difference between the contour points, λ_k, and the corresponding surface points, $\lambda(\mu_k, \theta_k)$. The second term is a smoothing function, which penalizes the bending energy of the surface,

$$S(\lambda)=\int_\Omega \left(\frac{\partial^2\lambda}{\partial\mu^2}\right)^2+2\left(\frac{\partial^2\lambda}{\partial\mu\partial\theta}\right)^2+\left(\frac{\partial^2\lambda}{\partial\theta^2}\right)^2 d\Omega$$

where Ω is the domain of the surface. 3D endocardial circumferential curvatures were then computed using standard formulas[21] at the wall segments[22] as previously defined (excluding the apex). Two-dimensional (2D) apex curvatures were computed as the average of apex curvatures calculated from endocardial contours drawn on 4-chamber view image and 2-chamber view image using standard formula.[21] Sphericity index was defined as the ratio of LV long-axis length to LV inner diameter.[23] Smaller sphericity index indicates greater sphericity. 3D wall thickness was computed at all wall segments[22] (excluding the apex) by measuring the 3D distance from a point on the epicardial surface to the closest point on the endocardial surface along a line perpendicular to the epicardial surface. Radius of curvature to wall thickness ratio (R/T) was computed by the reciprocal of the product of the endocardial circumferential curvature and 3D wall thickness.

Tagged MRI—Tagged MRI was acquired on the same scanner using the same slice prescription as cine MRI with the following typical parameters: repetition/echo times 8/4.2 ms, tag spacing 7 mm, trigger time 10 ms from R wave, flip angle 10^0. Tag lines were tracked[24] and edited, if necessary, by experts. LVES maximum shortening strain was computed at all wall segments (excluding the apex) by fitting a B-Spline deformation model in prolate-spheroidal coordinates to the tag line data.[25]

Bullet Formula—LVESV (ml) was also calculated based on LVESD (mm) and LVES length (cm) using the Bullet formula[26,27] as following,

$$\mathrm{LVESV}=0.83\times\pi\times\left(\frac{\mathrm{LVESD}}{20}\right)^2\times\mathrm{L}$$

where L is the length of LV measured from apex to the tip of the papillary muscle. This volume was referred to as calculated volume in the current study.

Statistical Analysis

Student's two sample *t* test (for continuous variables) and Fisher's exact test (for categorical variables) were conducted to compare the control group (n=51) and the MR group (n=94) in demographic, geometric and functional variables.

Regression analyses between LVESV and LVESD were performed in controls and MR. Model adequacy checking showed that the model was not linear for both groups. Therefore, square root transformation was performed to the control group which eliminated the non-linearity problem. For the MR group, square root transformation did not resolve the non-linearity problem. Thus, cubic root transformation was performed with which the test showed proof of linearity of the model. Student's pair *t* test was performed to compare the measured LVESV by summing up the volumes defined by contours multiplied by slice thickness versus calculated LVESV by the Bullet formula. Regression analysis was also

performed to test the association between the difference of measured and calculated LVESV and 3D distal LV circumferential curvature. Model adequacy checking showed that the model was not linear. Thus, square root transformation was performed which eliminated the non-linearity problem.

One-way analysis of variance (ANOVA) was used to perform group-wise comparisons among controls and MRs with LVESD < and ≥37mm (corresponding to > mean + 1 standard deviation of LVESD of the control group; moreover, mean LVESD in the MR group was equal to 37mm). The P values of all pair-wise differences were adjusted using the Tukey-Kramer procedure.

Comparisons of the MRI variables among controls and MRs before and 12 months after surgery were performed using a mixed model via PROC MIXED. The repeated measures of the MR patients before and after surgery were accounted for by an assumed compound symmetry correlation structure. To avoid inflating the probability of a Type I error, the Bonferroni-Holm step down test procedure was utilized to adjust the significance level accordingly.

Model adequacy checking was performed for all models. Linearity was checked by plotting the model residuals versus the dependent variable to look for any curve band or nonlinear pattern. Shapiro-Wilk test was performed for normality test. Log transformation, square root or cubic root transformation was performed if there were outliers, if the normality assumption was not valid, or if the homogeneity assumption was violated as appropriate. If the data transformation could not resolve the outlier problem, Wilcoxon's rank-sum test (for two groups' comparison) or Kruskal-Wallis test (for more than two groups' comparison) was performed.

Barnard's test[28, 29] was used to compare the post-operative incidence of LV dysfunction (defined as LVEF<50%) in patients with pre-operative LVESD <37mm vs. patients with pre-operative LVESD ≥ 37mm.

All data was presented as mean ± standard deviation (SD). A $P<0.05$ was considered statistically significant. We also conducted a general linear model for LV functional parameters to adjust for age and systolic BP using analysis of covariance. Age and systolic BP were considered as covariates. All statistical analysis was performed using SAS version 9.1.3.

Results

Clinical Characteristics

Clinical and MRI characteristics of the control subjects and 94 MR patients are outlined in Table 1. The two groups had a similar age range (20–70 and 25–76 years, respectively). However, the MR group was significantly older than the control. There were no significant differences in body surface area (BSA) and gender between the two groups. Heart rate, systolic and diastolic blood pressures (BP) were also similar in the two groups.

MRI-Derived Variables in Controls and MR Patients

As expected, MR patients had significant increases in LVEDV, LVESV, and LV stroke volume (SV) indices (volumes normalized to BSA), as well as higher LVED and LVES dimensions compared to controls. However, there were no differences in LV lengths at both ED and ES in MR patients vs. controls. MRI-derived LVEF was significantly different between the two groups. LV mass index and LVEDV/mass ratio were significantly

increased in MR vs. controls. Peak early filling rate was significantly higher in MR group vs. controls ($P < 0.0001$).

Figure 1A shows two representative examples from a control subject and a MR patient. Both hearts had the same LVESD (37mm) and similar LVES length; however, the MR LV had marked spherical remodeling demonstrated by the color coded circumferential curvature grid from base to distal LV depicted by lesser circumferential curvature (red) in the MR and greater circumferential curvature in the control (yellow). The LVESV of the MR heart was 85ml and that of the normal heart was 49ml. Figure 1B demonstrates LV remodeling in MR as compared to control.

Figure 2 demonstrates the relation between LVESV and LVESD in the MR (A) and control groups (B). In the MR group, this relation was cubic ($LVESV = (2 + 0.06 \times LVESD)^3$, $P<0.0001$) whereas this relation was quadratic in controls ($LVESV = (2.68 + 0.12 \times LVESD)^2$, $P<0.001$). Of particular interest, LVESV calculated based on LVESD using the Bullet formula demonstrated no significant difference from the measured LVESV by summated the serial short axis images in controls. However, the Bullet formula significantly underestimated LVESV in the MR group. This difference between the measured LVESV and the calculated LVESV in MR was significantly negative-correlated with the 3D circumferential curvature at distal LV ($P<0.0001$), as shown in Figure 2C.

Effect of LVESD on baseline LV geometry and function

All 94 MR patients were divided into two groups: 1) LVESD <37 mm, n=48 and 2) LVESD ≥37mm, n=46. The cut-off LVESD of 37mm was selected corresponding to > mean + 1 standard deviation of LVESD of the control group; Moreover, the mean LVESD of MR was equal to 37mm. Table 2 shows the comparisons between controls, and the two MR groups in LVES length, volume index, global and 2D apical sphericity. With LVESD < 37mm, there was no increase in length; however, LVESV, LV global and 2D apical sphericity were significantly higher than controls. With LVESD ≥37mm, LVESV was further increased while the apex curvature remained similarly lower than controls; with no commensurate increase in LV length, LV global sphericity was further increased.

Figure 3 demonstrates the differences in 3D LV geometry, and maximum shortening from base, mid, and distal LV at ED and ES among controls, MR with LVESD< and ≥37mm. In the MR patients, LVED circumferential curvature decreased and R/T ratio increased from base to distal LV vs. controls. These changes were more significant in MR ESD≥37mm than in MR ESD<37mm. In MR patients with LVESD ≥37mm, LVES circumferential curvature was significantly lower at LV base (0.44±0.04), mid (0.47±0.05), and distal LV (0.59±0.08) compared with MR ESD <37mm and controls ($P<0.0001$ for base, mid and distal LV). LVES R/T ratio was significantly increased in MR ESD ≥37mm (1.86±0.4 at base, 2.03±0.4 at mid and 2.01±0.5 at distal LV) compared with both MR ESD <37mm (1.48±0.3 at base, 1.67±0.4 at mid and 1.69±0.4 at distal LV, $P<0.0001$) and controls (1.64±0.4 at base, 1.61±0.4 at mid, 1.48±0.4 at distal LV, $P<0.0001$). However, in MR ESD<37mm, LVES R/T ratio did not differ from control at all segments. There were no significant differences among all three groups in LV maximum shortening strain after being adjusted for age and systolic BP.

LV Geometry and Function following MV repair

Table 3 shows the clinical characteristics of controls, pre-operative MR, and 12 months postoperative MR patients. The mean age of the surgical MR group was significantly higher and the percentage of females was significantly smaller in MR group vs. controls. Therefore, comparisons of LV functional parameters among the groups were adjusted for an age effect.

Controls and surgical MR patients before and after surgery had matched BSA, heart rate, systolic and diastolic BP. Before surgery, 20 patients were in New York Heart Association (NYHA) functional class I (57%), 14 patients were in NYHA class II (40%) and 1 patients were in NYHA class III (3%).

One year after the surgery, nearly all patients were classified as NYHA class I while one was NYHA class II. LVED dimension, LVEDV index, LV mass index were significantly decreased post-operatively, but remained greater than controls. LVEDV/mass returned to normal control level. Similarly, LVESD and LVESV index decreased post-operation but remained significantly greater than controls. Peak early filling rate was significantly increased prior to surgery and returned to lower than normal level after surgery. LVEF was decreased post-operatively compared to both controls and pre-operative MR.

Recovery after surgery in MR patients with LVESD < and ≥ 37 mm

The 35 surgical MR patients who underwent mitral valve repair were divided into two groups based on pre-operative LVESD < or ≥37mm. Figures 4 and 5 demonstrate the recovery of LV geometry after surgery at ED (Figure 4) and ES (Figure 5) in the MR patients. In MR with pre-operative LVESD <37mm, LVED circumferential curvature was decreased prior to and returned to normal after surgery. LVES circumferential curvature was decreased near distal LV prior to and normalized after surgery. LVED R/T ratio was normal before and after surgery, while LVES R/T ratio at base was significantly below normal but recovered after surgery. In MR patients with LVESD≥37mm, LVED and LVES circumferential curvatures were decreased prior to and improved after surgery, but remained below normal at ES. In contrast, the LVED R/T ratio returned to normal while LVES R/T ratio remained above controls after surgery.

Figure 6 shows the change in maximum shortening after surgery in the MR patients with LVESD < and ≥37mm. Although in MR ESD<37mm, LVES R/T ratio did not differ from controls before and after surgery, maximum shortening was significantly decreased from mid to distal LV after surgery. In MR ESD≥37mm, LVES maximum shortening was decreased at all levels after surgery.

Incidence of post-operative LV dysfunction

Table 4 shows that among the 35 surgical MR patients, 11 patients (31%) had post-operative LV dysfunction (defined as LVEF<50%). Two of them had pre-operative LVESD <37mm while night of them had pre-operative LVESD≥37mm. The incidence of post-operative LV dysfunction in MR ESD<37mm (14%) was lower than that in MR ESD≥37mm (43%, P=0.0616). There were ten surgical MR patients in LVESD range of 37 to 40mm and two of them (20%) had post-operative LV dysfunction.

Discussion

A major finding of the current investigation is that LVESD, although commonly used to assess the extent of LV remodeling in patients with isolated MR, does not accurately reflect the extent of LV remodeling, largely due to spherical LV remodeling from mid to apical LV. Furthermore, conservative management of patients with isolated MR based on standard dimensions was associated with significant decrease in LVEF and maximum strain post MV repair. In comparison to a group of control subjects with similar age range, the relation of LVESD to LVESV is cubic in MR in contrast to a quadratic relation in controls, indicating a greater increase in LVESV per unit of LVESD in MR as compared to controls. The Bullet formula, which is commonly used to calculate LV volumes, significantly underestimates MR LVESV based on the LVESD measured at the tips of the papillary muscles. The extra

volume can be attributed to the extensive LV mid to distal spherical remodeling, which is not accounted for in the Bullet formula. The importance of this finding is that while LVESD remains below the accepted target of 40 mm for surgical intervention of isolated MR, its associated LVESV can range as high as twice that of the normal controls. This finding therefore identifies a volumetric parameter (LVESV) that more suitably characterizes overall LV remodeling in isolated MR.

The variance in LVESV in MR is attributed to LV mid to apical spherical remodeling that is evident even in the patients with LVESD below 37mm; however, LVES R/T ratio remains normal suggesting a more compensated hypertrophy in this group. It is of interest that even with an increase in LVESV in the MR ESD ≥37mm group, there is not a commensurate LV elongation, which is consistent with a more global spherical LV remodeling. This is also associated with an increase in the LVES R/T ratio at all LV segments from base to distal LV, a marker of increased wall stress. Despite this progression of adverse LV remodeling, maximum shortening from the base to distal LV remains normal in both groups. This finding is in agreement with the known favorable loading conditions of an increase in LV preload and excessive adrenergic drive[30, 31] combined with a facilitation of ejection through a secondary ejection pathway into left atrium in isolated MR.

In an attempt to determine the functional importance of these geometric changes in isolated chronic MR, we evaluate LV geometry and function in 35 patients from this cohort before and one year after mitral valve repair. All patients are within current echocardiographic guidelines for mitral valve surgery for chronic MR. Nevertheless, LVEF are significantly decreased after surgery, despite normalization of the LVEDV/mass ratio. The incidence of postoperative LV dysfunction, defined as LVEF<50%, occurs in about 1/3rd of these patients. In particular, the incidence of post-operative LV dysfunction with LVESD≥37mm is greater than that with LVESD<37mm (P=0.0616). It is important to note that in MR patients with LVESD≥37mm, LVES R/T ratio remains ~30% above normal from mid to distal LV post-surgery. In addition, LV maximum shortening is decreased below normal from base to distal LV after surgery. Furthermore, in MR patients with LVESD<37 mm, the extent of spherical LV remodeling prior to surgery is associated with a significant decrease in LV maximum shortening after surgery. It is important to note that even in patients with MRI-derived LVEF>60% prior to mitral valve repair, directional changes after surgery remain the same (Supplemental Table 1, Supplemental Figure 1–3). The decrease in LVEF and LV maximum strain from pre- to postoperative values persists in patients with MRI-derived LVEF>60% prior to mitral valve repair (Supplemental Table 1, Supplemental Figure 3). We have recently reported the finding of excessive cardiomyocyte oxidative stress, myofibrillar degeneration, and lipofuscin accumulation, which collectively may result in irreversible cardiomyocyte dysfunction in patients with pre-operative LVEF >60%.[6] Taken together, the presence of adverse LV remodeling prior to MV surgery is associated with decreased maximal shortening one year after surgery.

Dujardin et al. have demonstrated an exponential correlation between LVESD and LVESV using echocardiography, especially for enlarged ventricles.[32] The current study utilizes MRI with 3D analysis and determines that the relation between LVESV and LVESD is cubic in MR and quadratic in controls. Apical spherical remodeling appears to occur prior to a significant change being detected at the base. Thus, severely elevated LVES volume can occur prior to LVES dimension reaching 40 mm. In support of a volumetric analysis in isolated MR, Ozdogan et al.[33] and Cawley et al. [34] have also suggested that the use of a geometry independent volume assessment using MRI is preferred for LVEF measurement in timing of surgery.

The current study is limited in that follow-up of patients is only one year in a small number of patients. Previous reports in patients with aortic regurgitation and aortic stenosis demonstrate that there is continued improvement for years following surgery.[35,36] Despite a small sample size, this represents a homogeneous population who do not have evidence of coronary artery disease by coronary angiography. All patients being referred for surgery had LVEF>60% and almost all had LVESD <40mm by referral echocardiography studies and need for surgery was based on conservative clinical judgment. Subsequent MRI and 3D analysis uncover some patients with LVEF<60%, highlighting the need for a more comprehensive volumetric analysis of LV remodeling. Finally, while we are convinced that the surrogate outcome of LVES volume will be strongly related with the important clinical outcomes, it is clear this question can only be addressed in a clinical trial testing the comparative effectiveness of LV dimensions versus MRI- or 3D echo-derived LV volume on clinical outcomes.

The results of the current study uncover greater LV remodeling that contributes to higher LVES volume and corresponds with decreased LV shortening strain after surgery, suggesting that simple geometry-based assessments of volume may underestimate LV dysfunction in isolated MR. The current investigation demonstrates the potential for high variability of spherical remodeling from the LV mid to apex, beyond the conventional point of LVESD measurement, that contributes to the increase of LVES volume. Importantly, this adverse LV remodeling prior to surgery is associated with a reduction in maximum shortening. These results suggest that a more detailed geometric LV analysis and volume based assessment at ES provide a superior evaluation of extent of LV remodeling and may serve as a better marker for optimal timing of surgery in the patient with isolated MR in order to maximally preserve post-operative LV function.

Supplementary Material

Refer to Web version on PubMed Central for supplementary material.

Acknowledgments

Funding Sources: This work was supported by NIH Specialize Center of Clinically Oriented Research in Cardiac Dysfunction P50-HL077100.

References

1. Nkomo VT, Gardin JM, Skelton TN, Gottdiener JS, Scott CG, Enriquez-Sarano M. Burden of valvular heart diseases: a population-based study. Lancet. 2006; 368:1005–1011. [PubMed: 16980116]
2. Enriquez-Sarano M, Akins CW, Vahanian A. Mitral regurgitation. Lancet. 2009; 373:1382–1394. [PubMed: 19356795]
3. Enriquez-Sarano M, Tajik AJ, Schaff HV, Orszulak TA, McGoon MD, Bailey KR, Frye RL. Echocardiographic prediction of left ventricular function after correction of mitral regurgitation: results and clinical implications. J Am Coll Cardiol. 1994; 24:1536–1543. [PubMed: 7930287]
4. Borer JS, Bonow RO. Contemporary approach to aortic and mitral regurgitation. Circulation. 2003; 108:2432–2438. [PubMed: 14623790]
5. Bonow RO, Carabello BA, Chatterjee K, de Leon AC Jr, Faxon DP, Freed MD, Gaasch WH, Lytle BW, Nishimura RA, O'Gara PT, O'Rourke RA, Otto CM, Shah PM, Shanewise JS, Smith SC Jr, Jacobs AK, Adams CD, Anderson JL, Antman EM, Fuster V, Halperin JL, Hiratzka LF, Hunt SA, Lytle BW, Nishimura R, Page RL, Riegel B. ACC/AHA 2006 guidelines for the management of patients with valvular heart disease: a report of the American College of Cardiology/American Heart Association Task Force on Practice Guidelines (writing Committee to Revise the 1998 guidelines for the management of patients with valvular heart disease) developed in collaboration

with the Society of Cardiovascular Anesthesiologists endorsed by the Society for Cardiovascular Angiography and Interventions and the Society of Thoracic Surgeons. J Am Coll Cardiol. 2006; 48:e1–148. [PubMed: 16875962]

6. Ahmed M, Gladden JD, Litovsky S, McGiffin D, Gupta H, Lloyd S, Denney T, Dell'Italia LJ. Myofibrillar degeneration, oxidative stress and post surgical systolic dysfunction in patients with isolated mitral regurgitation and pre surgical LV ejection fraction > 60%. J Am Coll Cardiol. 2010; 55:671–679. [PubMed: 20170794]
7. Adams DH, Rosenhek R, Falk V. Degenerative mitral valve regurgitation: best practice revolution. Eur Heart J. 2010; 31:1958–1966. [PubMed: 20624767]
8. Samad Z, Kaul P, Shaw LK, Glower DD, Velazquez EJ, Douglas PS, Jollis JG. Impact of early surgery on survival of patients with severe mitral regurgitation. Heart. 2011; 97:221–224. [PubMed: 21071750]
9. Kang DH, Kim JH, Rim JH, Kim MJ, Yun SC, Song JM, Song H, Choi KJ, Song JK, Lee JW. Comparison of early surgery versus conventional treatment in asymptomatic severe mitral regurgitation. Circulation. 2009; 119:797–804. [PubMed: 19188506]
10. Crawford MH, Souchek J, Oprian CA, Miller DC, Rahimtoola S, Giacomini JC, Sethi G, Hammermeister KE. Determinants of survival and left ventricular performance after mitral valve replacement. Department of Veterans Affairs Cooperative Study on Valvular Heart Disease. Circulation. 1990; 81:1173–1181. [PubMed: 2317900]
11. Zile MR, Gaasch WH, Carroll JD, Levine HJ. Chronic mitral regurgitation: predictive value of preoperative echocardiographic indexes of left ventricular function and wall stress. J Am Coll Cardiol. 1984; 3:235–42. [PubMed: 6693615]
12. Schuler G, Peterson KL, Johnson A, Francis G, Dennish G, Utley J, Daily PO, Ashburn W, Ross J Jr. Temporal response of left ventricular performance to mitral valve surgery. Circulation. 1979; 59:1218–1231. [PubMed: 436214]
13. Flemming MA, Oral H, Rothman ED, Briesmiester K, Petrusha JA, Starling MR. Echocardiographic markers for mitral valve surgery to preserve left ventricular performance in mitral regurgitation. Am Heart J. 2000; 140:476–482. [PubMed: 10966551]
14. Lindmark K, Söderberg S, Teien D, Näslund U. Long-term follow-up of mitral valve regurgitation--Importance of mitral valve pathology and left ventricular function on survival. Int J Cardiol. 2009; 137:145–150. [PubMed: 18707770]
15. Matsumura T, Ohtaki E, Tanaka K, Misu K, Tobaru T, Asano R, Nagayama M, Kitahara K, Umemura J, Sumiyoshi T, Kasegawa H, Hosoda S. Echocardiographic prediction of left ventricular dysfunction after mitral valve repair for mitral regurgitation as an indicator to decide the optimal timing of repair. J Am Coll Cardiol. 2003; 42:458–463. [PubMed: 12906972]
16. Enriquez-Sarano M, Avierinos JF, Messika-Zeitoun D, Detaint D, Capps M, Nkomo V, Scott C, Schaff HV, Tajik AJ. Quantitative determinants of the outcome of asymptomatic mitral regurgitation. N Engl J Med. 2005; 352:875–883. [PubMed: 15745978]
17. Montant P, Chenot F, Robert A, Vancraeynest D, Pasquet A, Gerber B, Noirhomme P, El Khoury G, Vanoverschelde JL. Long-term survival in asymptomatic patients with severe degenerative mitral regurgitation: a propensity score-based comparison between an early surgical strategy and a conservative treatment approach. J Thorac Cardiovasc Surg. 2009; 138:1339–1348. [PubMed: 19660385]
18. Rosenhek R, Rader F, Klaar U, Gabriel H, Krejc M, Kalbeck D, Schemper M, Maurer G, Baumgartner H. Outcome of watchful waiting in asymptomatic severe mitral regurgitation. Circulation. 2006; 113:2238–2244. [PubMed: 16651470]
19. Feng W, Nagaraj H, Gupta H, Lloyd SG, Aban I, Perry GJ, Calhoun DA, Dell'Italia LJ, Denney TS Jr. A dual propagation contours technique for semi-automated assessment of systolic and diastolic cardiac function by CMR. J Cardiovasc Magn Reson. 2009; 11:30. [PubMed: 19674481]
20. Young AA, Orr R, Smaill BH, Dell'Italia LJ. Three-dimensional changes in left and right ventricular geometry in chronic mitral regurgitation. Am J Physiol. 1996; 271:H2689–700. [PubMed: 8997332]
21. Lipshultz, M. Schaum's Outline of Differential Geometry. 1. New York: McGraw-Hill; 1969.

22. Cerqueira MD, Weissman NJ, Dilsizian V, Jacobs AK, Kaul S, Laskey WK, Pennell DJ, Rumberger JA, Ryan T, Verani MS. American Heart Association Writing Group on Myocardial Segmentation and Registration for Cardiac Imaging. Standardized myocardial segmentation and nomenclature for tomographic imaging of the heart. Int J Cardiovasc Imaging. 2002; 18:539–549. [PubMed: 12135124]

23. Di Donato M, Dabic P, Castelvecchio S, Santambrogio C, Brankovic J, Collarini L, Joussef T, Frigiola A, Buckberg G, Menicanti L. RESTORE Group. Left ventricular geometry in normal and post-anterior myocardial infarction patients: Sphericity index and 'new' conicity index comparisons. Eur J Cardiothorac Surg. 2006; 29:S225–230. [PubMed: 16564696]

24. Denney TS Jr, Gerber BL, Yan L. Unsupervised reconstruction of a three dimensional left ventricular strain from parallel tagged cardiac images. Magn Reson Med. 2003; 49:743–754. [PubMed: 12652546]

25. Li J, Denney TS. Left ventricular motion reconstruction with a prolate spheroidal B-spline model. Phys Med Biol. 2006; 51:517–537. [PubMed: 16424579]

26. Wyatt HL, Heng MK, Meerbaum S, Gueret P, Hestenes J, Dula E, Corday E. Cross-sectional echocardiography. II. Analysis of mathematic models for quantifying volume of the formalin-fixed left ventricle. Circulation. 1980; 61:1119–1125. [PubMed: 7371124]

27. Dell'Italia LJ, Blackwell GG, Pearce DJ, Thorn B, Pohost GM. Assessment of ventricular volumes using cine magnetic resonance in the intact dog. A comparison of measurement methods. Invest Radiol. 1994; 29:162–167. [PubMed: 8169091]

28. Barnard GA. Significance Tests for 2 × 2 tables. Biometrika. 1947; 34:156–177.

29. Mehta, CR.; Senchaudhuri, P. [Accessed September 4, 2003.] Conditional versus unconditional exact tests for comparing two binomials. http://www.cytel.com/papers/twobinomials.pdfUpdated September 4, 2003

30. Mehta RH, Supiano MA, Oral H, Grossman PM, Montgomery DS, Smith MJ, Starling MR. Compared with control subjects, the systemic sympathetic nervous system is activated in patients with mitral regurgitation. Am Heart J. 2003; 145:1078–1085. [PubMed: 12796766]

31. Sabri A, Rafiq K, Seqqat R, Kolpakov MA, Dillon R, Dell'italia LJ. Sympathetic activation causes focal adhesion signaling alteration in early compensated volume overload attributable to isolated mitral regurgitation in the dog. Circ Res. 2008; 102:1127–1136. [PubMed: 18356543]

32. Dujardin KS, Enriquez-Sarano M, Rossi A, Bailey KR, Seward JB. Echocardiographic assessment of left ventricular remodeling: are left ventricular diameters suitable tools? J Am Coll Cardiol. 1997; 30:1534–1541. [PubMed: 9362413]

33. Ozdogan O, Yuksel A, Gurgun C, Kayikcioglu M, Yavuzgil O, Cinar CS. Assessment of cardiac remodeling in asymptomatic mitral regurgitation for surgery timing: a comparative study of echocardiography and magnetic resonance imaging. Cardiovasc Ultrasound. 2010; 8:32. [PubMed: 20704764]

34. Cawley PJ, Otto CM. Valvular regurgitation: does cardiovascular magnetic resonance provide additional information compared to echocardiography? Minerva Cardioangiol. 2009; 57:521–535. [PubMed: 19763073]

35. Borer JS, Herrold EM, Hochreiter C, Roman M, Supino P, Devereux RB, Kligfield P, Nawaz H. Natural history of left ventricular performance at rest and during exercise after aortic valve replacement for aortic regurgitation. Circulation. 1991; 84:III133–139. [PubMed: 1934401]

36. Villari B, Vassalli G, Monrad ES, Chiariello M, Turina M, Hess OM. Normalization of diastolic dysfunction in aortic stenosis late after valve replacement. Circulation. 1995; 91:2353–2358. [PubMed: 7729021]

Clinical Commentary

Although surgery is indicated in patients with mitral regurgitation (MR) when left ventricular (LV) end-systolic (ES) dimension is >40mm, LV ejection fraction (EF) may decrease post-mitral valve surgery. A major finding of the current investigation is that LVES dimension does not accurately reflect the extent of LV remodeling, largely due to spherical LV remodeling from mid to apical LV by MRI with three-dimensional (3D) analysis. This study demonstrates that even when LVES dimension remains below the accepted target of 40 mm for surgical intervention of isolated MR, its associated LVES volume can range as high as twice that of the normal controls. MRI with 3D analysis or 3D echocardiography derived LV volumes may be preferred to evaluate disease progression in isolated MR.

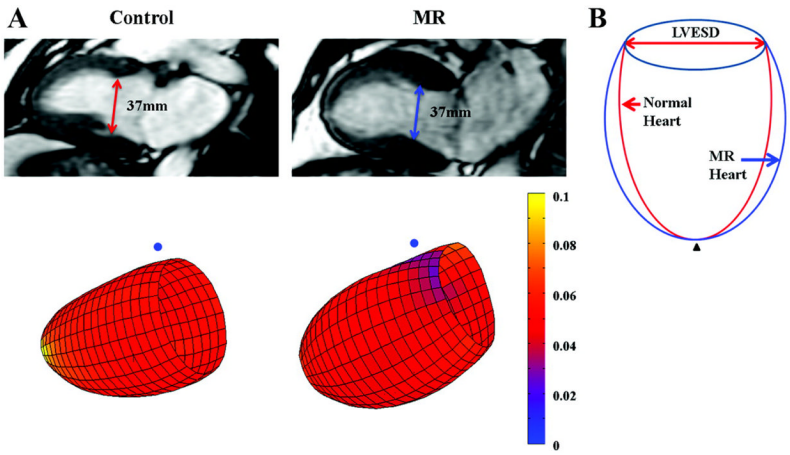

Figure 1.

(A) Representative LV end-systolic (ES) with two chamber view (top row) and 3-dimensional surface representations (bottom row) using color scales of LVES endocardial surface circumferential curvature (1/mm) from a control subject and a MR patient; **(B)** Systematic simulation of MR LV remodeling with respect to control. The MR heart has the same LVES dimension and similar long axis length as control. However, there is lesser curvature from the mid to distal LV segments represented by a dimmer red color in the MR patient vs. control (brigher yellow color). These changes in the MR patient contribute to a more spherical LV remodeling and a larger LVES volume. Blue dot: mid-septum; black triangle: apex.

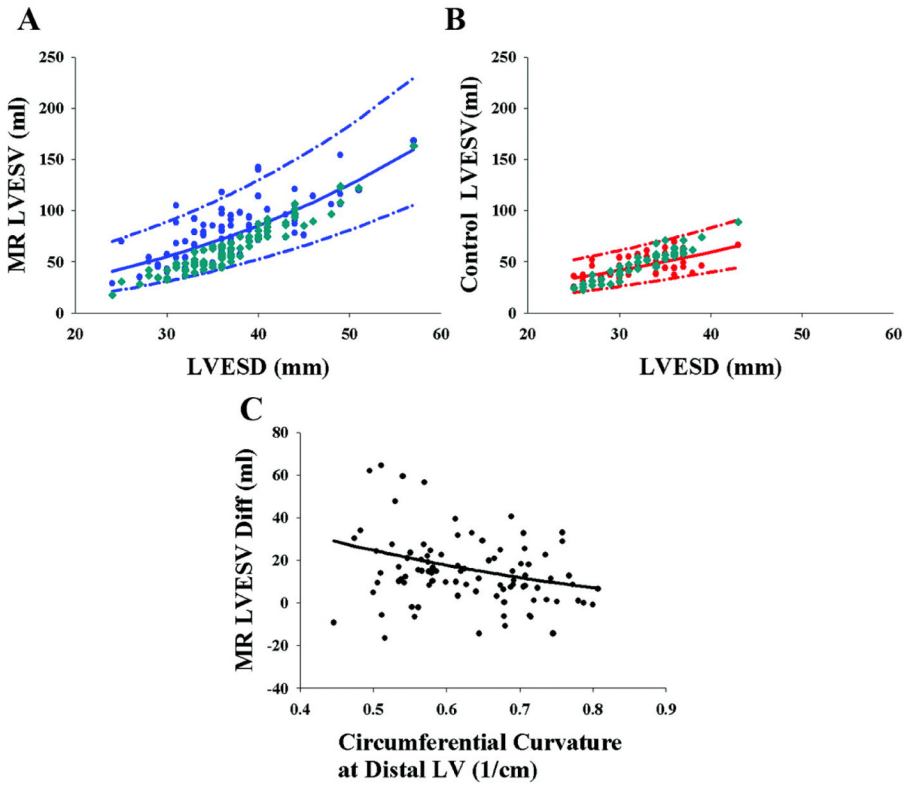

Figure 2.

Correlation between LVESV and LVESD in MR patients **(A)** and control subjects **(B)**. The solid lines represent the fitted model for the LVESD vs. LVESV relation with 95% confidence intervals (dash lines), which is cubic in MR patients (n=94) and quadratic in controls (n =51). Data of calculated LVESV using the Bullet formula are shown as dark cyan points in (A) and (**B**). The difference between the measured LVESV from summated short axis images and calculated LVESV from Bullet formula in MR were plotted in **(C)** vs. LVES circumferential curvature at distal LV. The solid back line in (**C**) represents the fitted model.

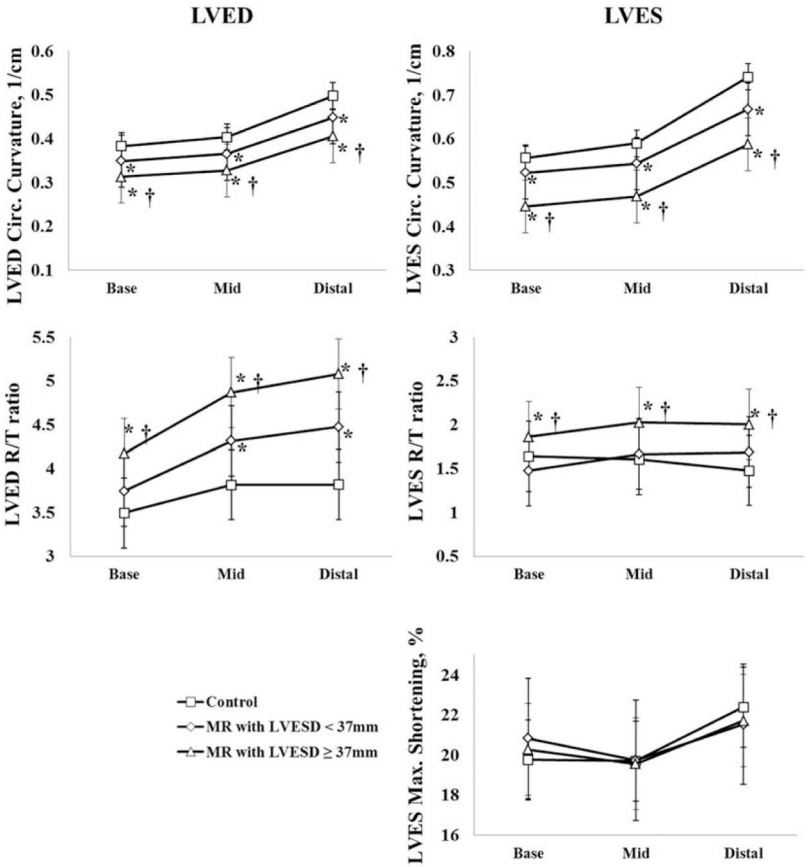

Figure 3.

Three-dimensional LVED (left column) and LVES (right column) geometry with maximum shortening in the controls (n=51) and MR patients (n=94) divided into those with LVESD <37 mm and LVESD ≥37 mm. These data demonstrate progressive global LVED and LVES remodeling in both groups of MR patients compared to controls. However, LV maximum shortening remains normal or even supra-normal in both MR groups. *: P<0.05 vs. controls; †: P<0.05 vs. MR patients with pre-operative LVESD<37 mm.

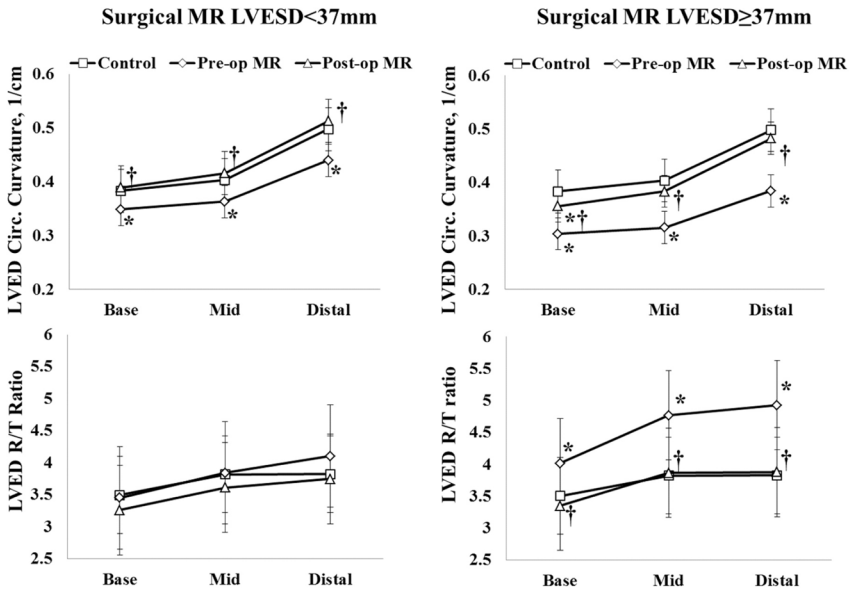

Figure 4.

Comparison of LV end-diastolic (ED) geometric remodeling in controls and in surgical MR patients with pre-operative LVESD < and ≥ 37mm before and after surgery. These data demonstrate progressive LV remodeling at ED in the two MR groups and their recovery after surgery. LVED R/T ratio is normalized after surgery in both MR groups. Circumferential curvatures in MR LVESD<37mm are normalized after surgery while in MR LVESD≥37mm, circumferential curvatures are increased yet not normalized. *: P<0.05 vs. controls; †: P<0.05 vs. pre-operative MR.

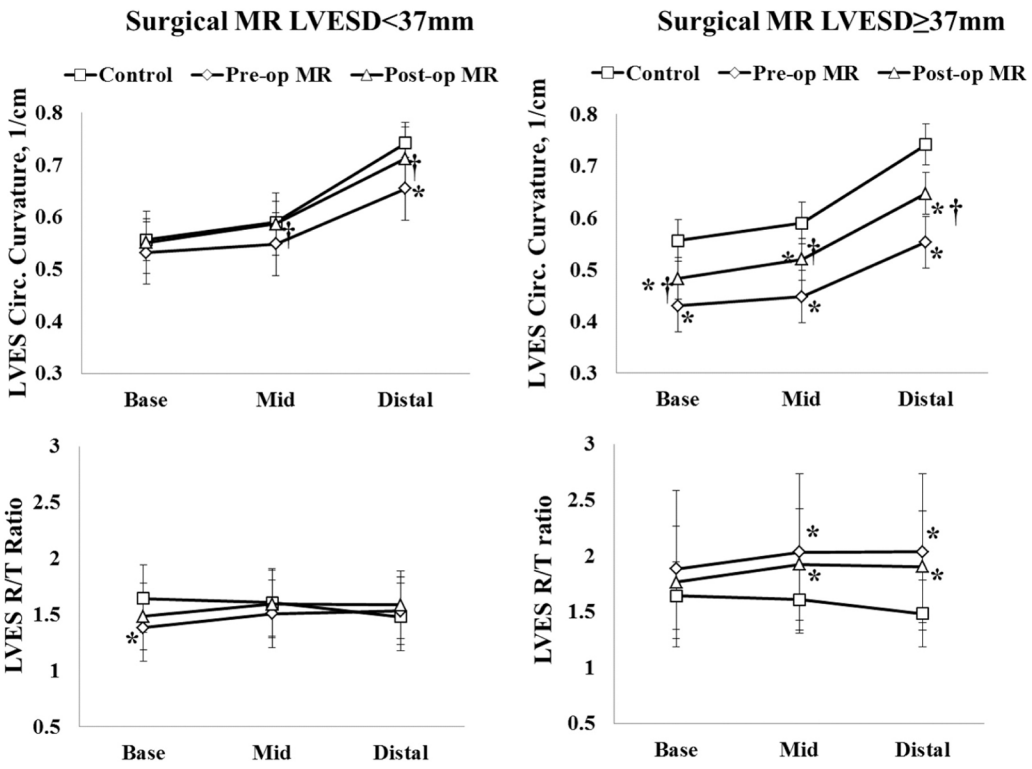

Figure 5.

Comparison of LV end-systolic (ES) geometric remodeling in controls and in surgical MR patients with pre-operative LVESD < and ≥ 37mm before and after surgery. These data demonstrate progressive LV remodeling at ES that is not normalized after surgery in the MR patients with pre-operative LVESD ≥37mm, while it is normalized after surgery in MR patients with pre-operative LVESD <37mnm. *: P<0.05 vs. controls; †: P<0.05 vs. pre-operative MR.

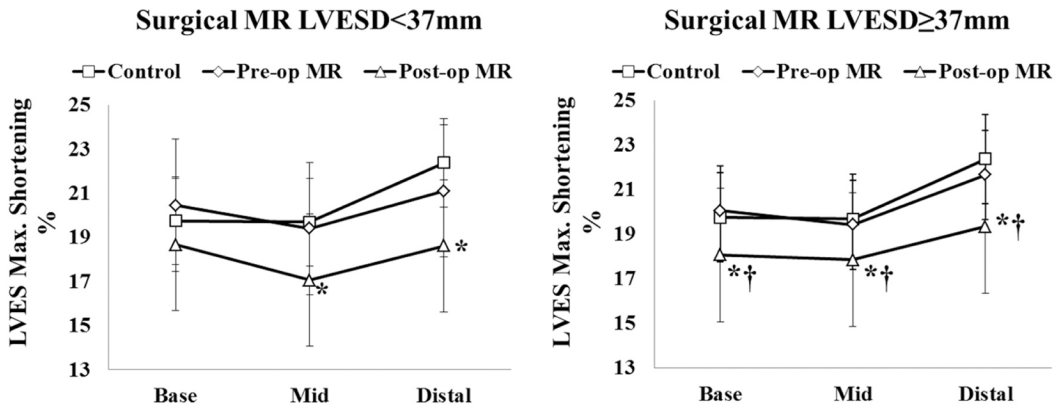

Figure 6.

Comparison of LV end-systolic (ES) maximum shortening in controls and in surgical MR patients with pre-operative LVESD < and ≥ 37mm before and after surgery. These data demonstrate that maximum shortening is decreased below normal in both groups of MR patients except that LVES maximum shortening is preserved at the base in patients with pre-operative LVESD <37 mm. *: P<0.05 vs. controls; †: P<0.05 vs. pre-operative MR.

Table 1

Baseline demographic and MRI characteristics of controls and MR patients

	Control (n=51)	MR (n=94)
Age, year	44±14	54±11*
Age range, year	20–70	25–76
% Female	53	38
Body Surface Area, m^2	1.91±0.24	1.92±0.22
Heart rate, beats/min	67±12	68±11
Systolic BP, mm Hg†	118±13	124±15
Diastolic BP, mm Hg†	75±10	76±9
LVEDV index, ml/m^2†	69±10	105±24*
LVESV index, ml/m^2†	25±6	41±13*
LVSV index, ml/m^2†	44±7	64±16*
LVEF, %	64±6	61±7*
LVED dimension, mm	49±4	58±6*
LVES dimension, mm†	32±4	37±6*
LVED length, cm	8.82±0.81	8.99±0.91
LVES length, cm	6.82±0.86	6.93±0.82
LV ED Mass index, g†	50±10	64±17*
LVEDV/Mass, ml/g†	1.45±0.38	1.68±0.34*
Peak early filling rate, ml/sec†	378±110	518±240*

Values are mean±SD. BP: blood pressure; LV: left ventricle; EDV: end-diastolic volume; ESV: end-systolic volume; EF: ejection fraction;

*$P < 0.05$ vs. controls;

†log transformation was performed.

Table 2

LV Geometry in MR patients with LVESD < 37 mm and ≥ 37 mm

	Control (n=51)	MR	
		LVESD<37mm (n=48)	LVESD≥37mm (n=46)
LVES length, cm	6.81±0.86	6.73±0.87	7.14±0.69†
LVES sphericity index	1.95±0.26	1.82±0.23*	1.64±0.21*†
LVES volume index, ml/m²	25±6	34±9*	48±13*†
2D LV apex curvature, 1/cm‡	2.93±1.13	1.89±0.48*	1.84±1.54*

Values are mean±SD.

*P<0.05 vs. controls;

†P<0.05 vs. MR patients with LVESD<37 mm;

‡log transformation was performed.

Table 3

Clinical characteristics of surgical patients with MV repair

	Control (n=51)	MR	
		Pre-operative (n=35)	Post-operative (n=35)
Age, year	44±14	53±11*	54±11*
% Female	53	20*	20*
Body surface area, m^2	1.9±0.24	2.00±0.24	1.98±0.23
Heart rate, beats/min	67±12	71±11	69±10
Systolic BP, mm Hg‡	118±13	124±15	121±11
Diastolic BP, mm Hg	75±10	78±8	76±10
LV ED volume index, ml/m^2‡	69±10	112±24*	80±18*†
LV ES volume index, ml/m^2‡	25±7	45±13*	38±14*†
LV SV volume index, ml/ m^2‡	44±7	67±16*	42±8†
LV EF, %	64±7	61±7*	54±8*†
LV ED dimension, mm‡	49±4	60±7*	51±6*†
LV ES dimension, mm‡	32±4	39±6*	36±7*†
LV ED mass index, g/m^2	50±10	67±14*	57±13*†
LV ED volume/mass, ml/g	1.45±0.38	1.70±0.35*	1.45±0.38†
LV ES R/T ratio‡	1.48±0.40	1.84±0.60*	1.78±0.68*
Peak early filling rate, ml/sec‡	378±110	632±270*	285±96*†

Values are n or mean±SD. BP: blood pressure; R/T ratio: radius /wall thickness measured at distal LV;

*P<0.05 vs. control;

†P<0.05 vs. pre-operative MR;

‡log transformation was performed.

Table 4

Stratification of pre-operative LVESD for post-operative LV dysfunction

Post-operative	Pre-operative LVESD	
	<37 mm	**≥37 mm**
Total, n	14	21
LVEF<50%, n	2	9
Incidence of LV dysfunction, %	14%	43%*

* P = 0.0616 vs. MR patients with pre-operative LVESD <37mm;